Electronic Supplementary Material (ESI) for Physical Chemistry Chemical Physics.

Charge-Transfer Complexation Between Naphthalene Diimides and Aromatic Solvents

Supporting Information

Chidambar Kulkarni,[a,b] Ganga Periyasamy,[b]
S. Balasubramanian[b*] Subi J. George[a*1]

[a] *Supramolecular Chemistry Lab, New Chemistry Unit, Jawaharlal Nehru Center for Advanced Scientific Research (JNCASR), Bangalore-560064, India , email: george@jncasr.ac.in*

[b] *Chemistry and Physics of Materials Unit, JNCASR, Bangalore-560064 India , email: bala@jncasr.ac.in*

Table of Contents

1 Experimental details

Electronic absorption spectra were recorded on a Perkin Elmer Lambda 900 UV-Vis-NIR spectrometer. Emission spectra were recorded on a Perkin Elmer LS 55 luminescence spectrometer. Temperature-dependent UV/Vis absorption and emission studies were performed using a Perkin Elmer LS 55 with a PTP-1 and Lambda 750 attached to PTP-1+1 Peltier system respectively. Jasco J-815 spectrometer was used to measuree Circular Dichroism (CD) spectra with a standard sensitivity (100 mdeg), scan rate of 100 nm/minute, bandwidth vaule of 1 and single accumulation for each spectra. Time-Correlated Single Photon Counting (TCSPC) experiments were performed using FLSP 920 spectrometer, Edinburgh Intrument. EPLED source of 380 nm was used for excitation. Unless otherwise mentioned all the optical studies were performed in 10 mm path length cuvettes. Fluorescence quantum yield was calculated using Quinine sulphate dihydrate as the standard with a quantum yield of 0.577 at an excitation of 350 nm using the standard formula.[1] The integrated area was calculated for all spectra from 370 nm to 650 nm. The solvent polarity parameter $E_T(30)$[2] was used to analyze the influence of solvent polarity on the observed fluorescence spectral changes. ^{1}H-NMR spectra were recorded on a Bruker AVANCE-400 spectrometer operating at 400 MHz at 27 °C.

2 Computational details

Time-Dependent Density-Functional Theory (TD-DFT) studies were performed to understand the origin of changes observed in the experimantal UV/Vis absorption spectra of **1** and **2** in different aromatic solvents. Geometry optimization of model compound (**1′**; obtained by replacing cholesterol in **1** by methyl groups) and the complex of **1′** with four molecules of different aromatic molecules was carried out using periodic density functional theory and the QUICKSTEP module[3] as implemented in CP2K package.[4]

Combined atom centered and plane wave basis sets were used to carry out geometry optimization. BLYP exchange-correlation functional,[5,6] double-zeta single polarized basis set[7] and Grimme's empirical dispersion correction (D3)[8] were used for geometry optimization. Goedecker-Teter-Hutter pseudopotential[9,10] to describe the effect of core electrons on the nuclei and an energy cut-off of 280 Ry was used. A cubical box length of 32 Åwas used for all the systems. LBFGS optimizer[11] and Wavelet poission solver was used for all geometry optimizations. Vertical transitions were calculated on optimized geometries at B3LYP/6-31+G(d,p) level of theory for 24 states using Gaussian-09.[12] The molecular orbtials were visualized suing GaussView 5.0.[13]

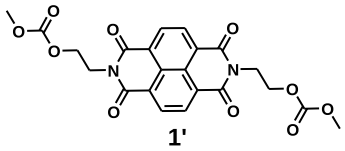

1'

3 Supporting Figures

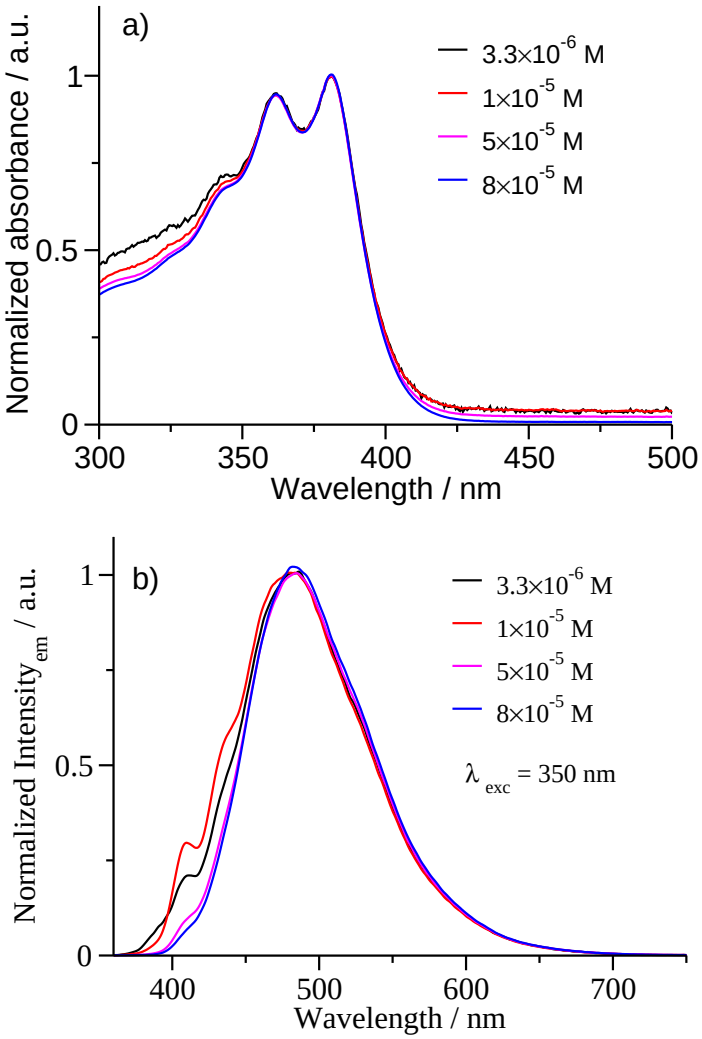

Figure S1: a) and b) Normalized UV/Vis absorption and emission spectra respectively of **1** in toluene at different concentrations

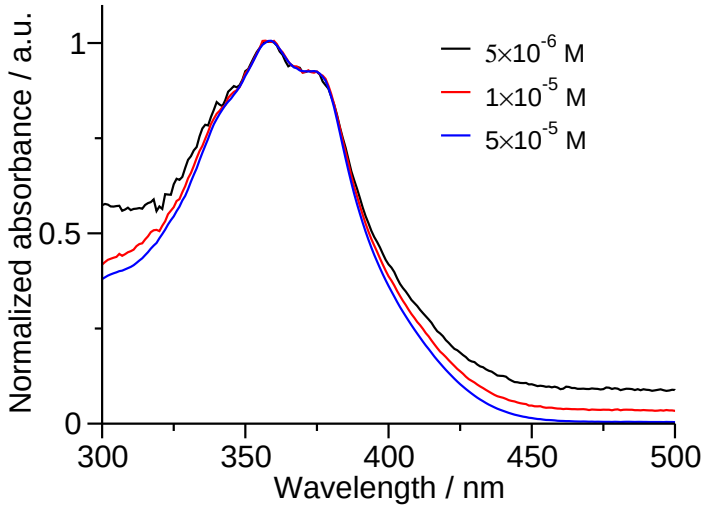

Figure S2: Concentration dependent absorption spectra of **1** in mesitylene

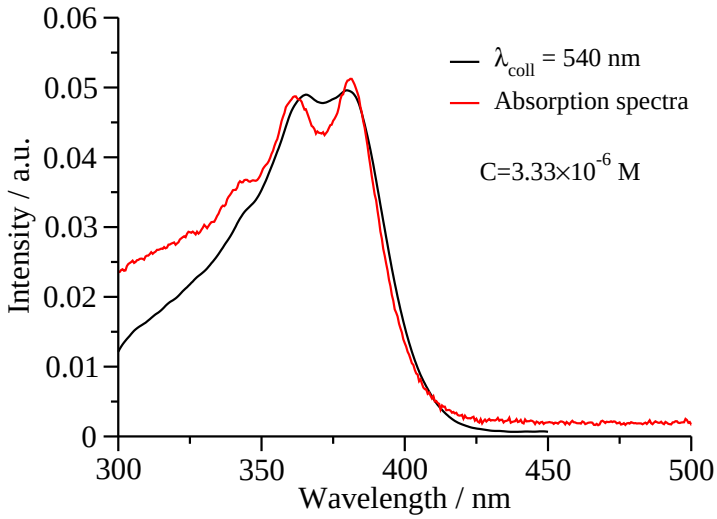

Figure S3: Excitation spectra of **1** in toluene overlapped with the corresponding UV/Vis absorption spectra (c = 3.3×10^{-6} M)

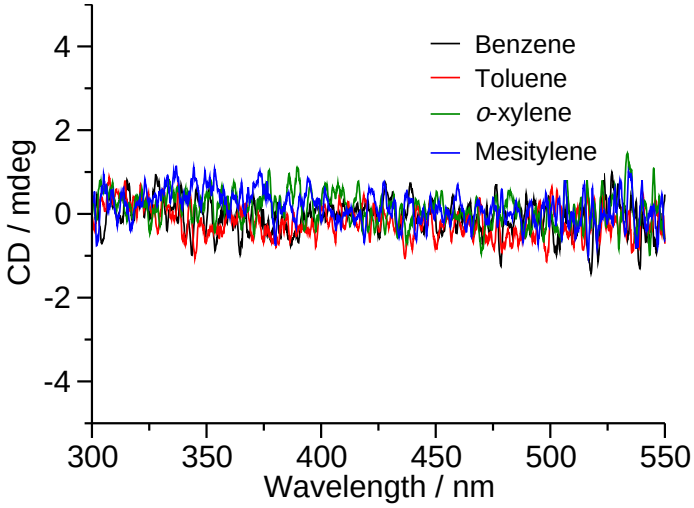

Figure S4: CD spectra of **1** in different aromatic solvents (c = 5×10^{-5} M)

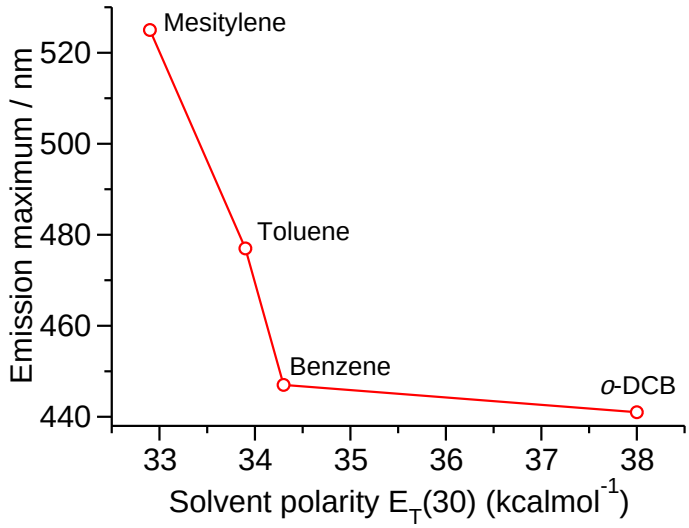

Figure S5: Variation of emission maximum of **1** versus the solvent polarity of the corresponding solvents

The emission maximum red-shifts with decrease in the solvent polarity. Thus the observed spectral shifts cannot be explained based on the solvent polarity.

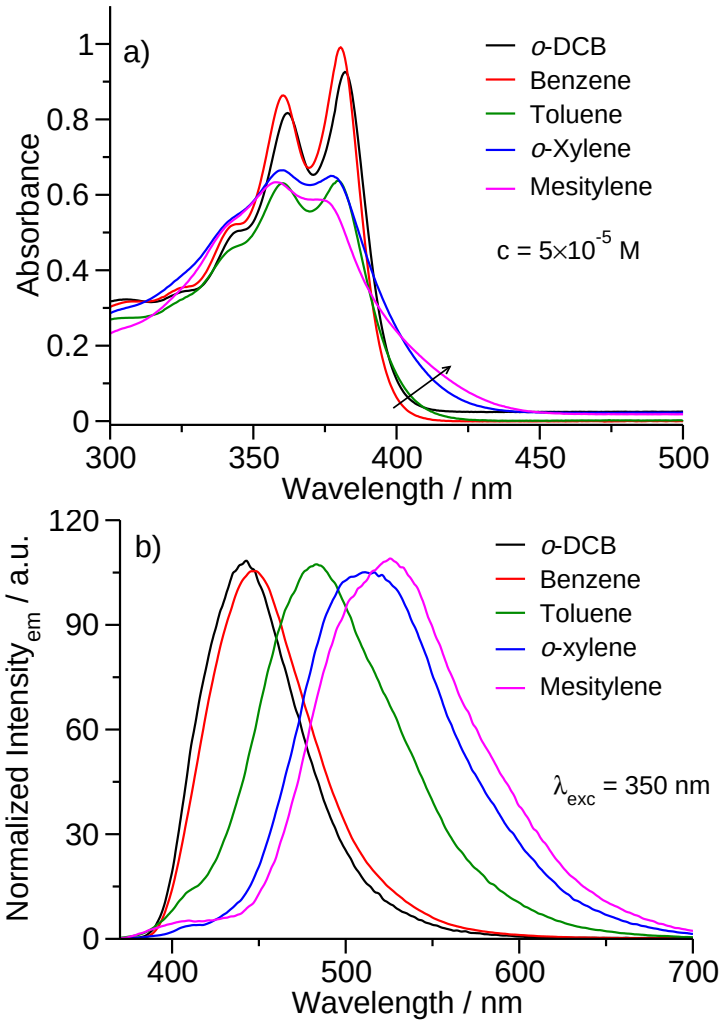

Figure S6: a) and b) UV/Vis absorption and emission spectra respectively of **2** in different aromatic solvents (c = 5×10^{-5} M)

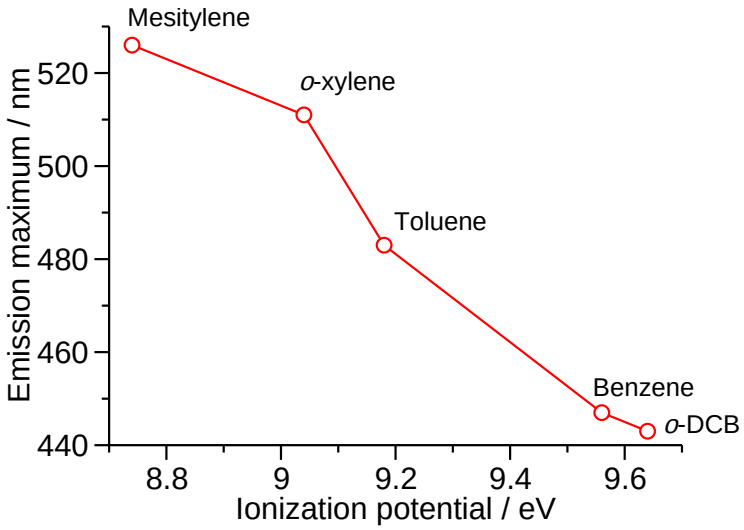

Figure S7: Variation of emission maximum of **2** versus the ionization potential of the corresponding solvents

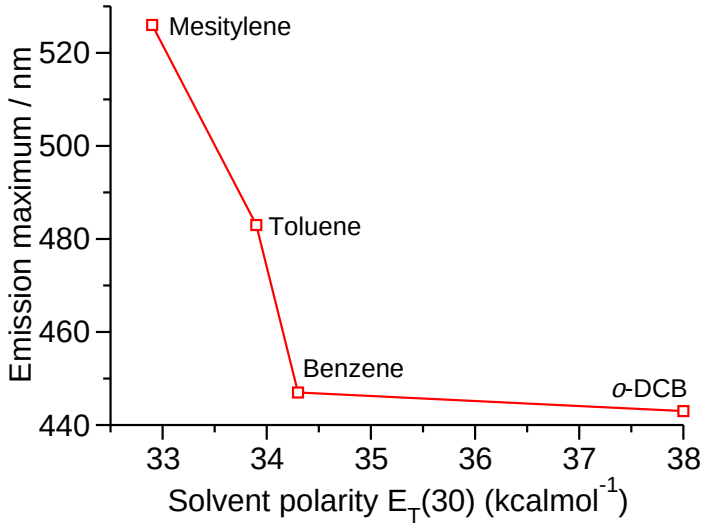

Figure S8: Variation of emission maximum of **2** versus the solvent polarity of the corresponding solvents

The emission maximum red-shifts with decrease in the solvent polarity. Thus the observed shifts cannot be explained based on the solvent polarity.

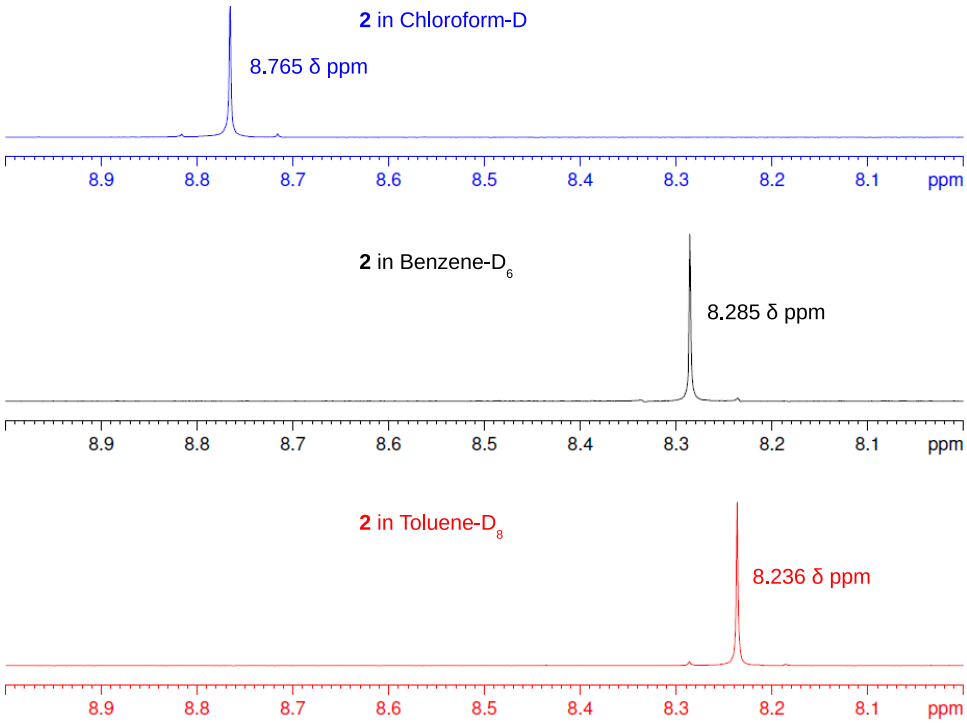

Figure S9: Partial ^{1}H-NMR spectra of **2** in different solvents (c = 2.5×10^{-3} M)

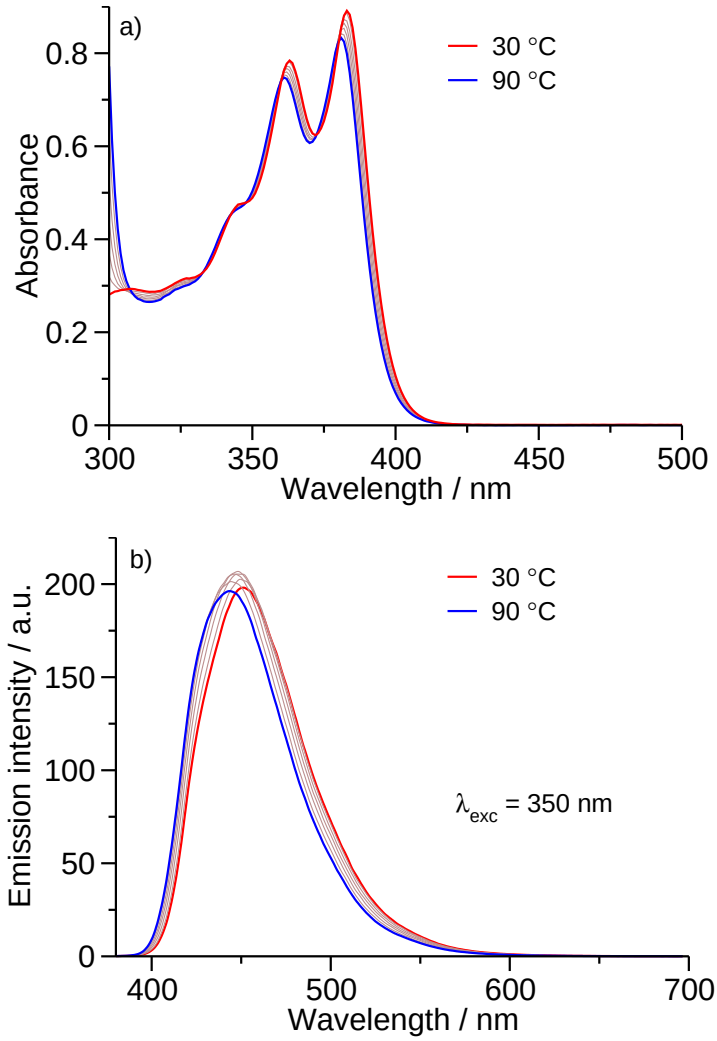

Figure S10: Temperature-dependent UV/Vis absorption (a) and emission spectra (b) of **2** in *o*-DCB at every 10 °C (c = 5×10^{-5} M)

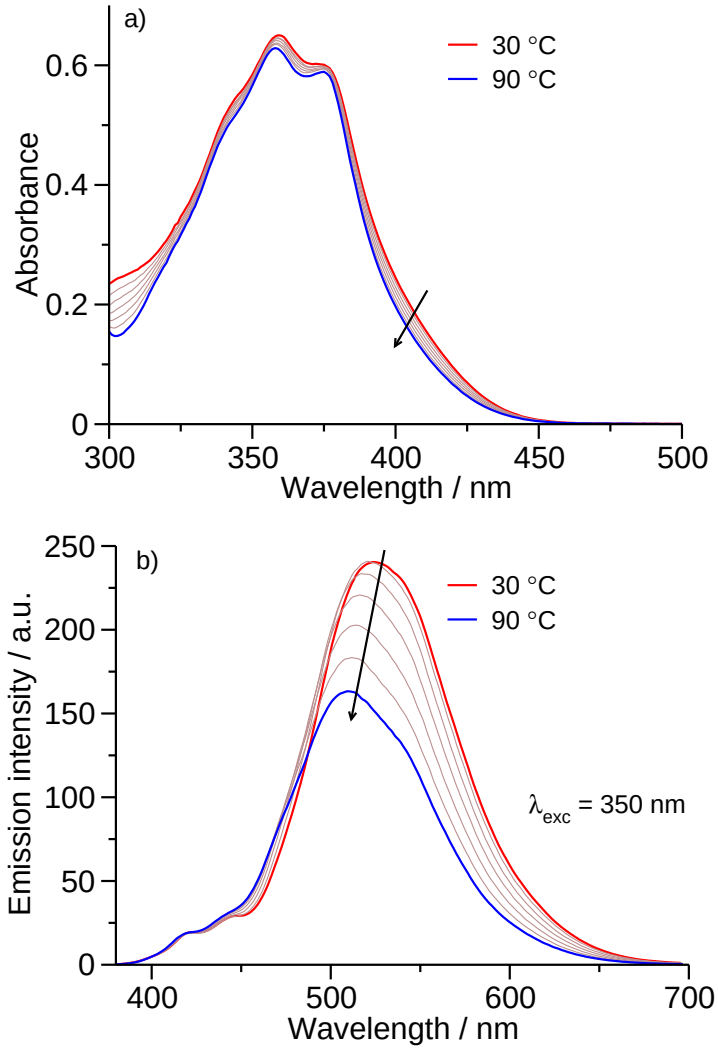

Figure S11: Temperature-dependent UV/Vis absorption (a) and emission spectra (b) of **2** in mesitylene at every 10 °C (c = 5×10^{-5} M). Arrows indicates spectral changes with increase in temperature.
Although the emission intensity decrease with increase in temperature, monomeric emission (at 410 nm) does not increase. This observation suggestions that CT complex is not dissociated at even higher temperatures.

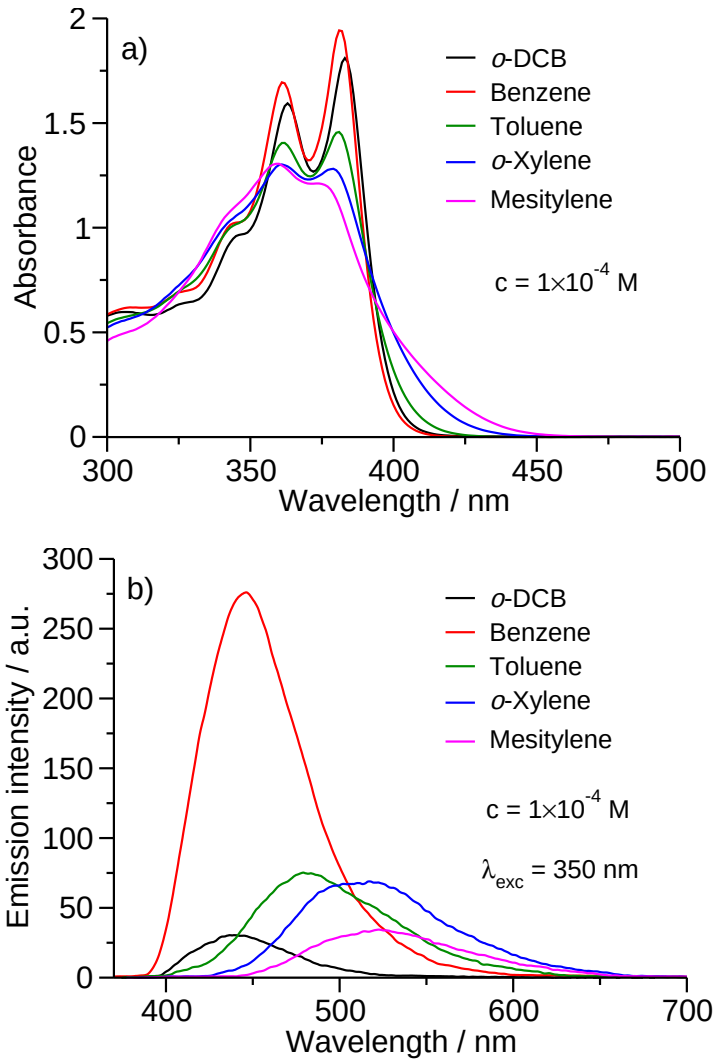

Figure S12: a) and b) UV/Vis absorption and emission spectra of **2** respectively in different aromatic solvents (c = 1×10^{-4} M)

The lack of any scattering at higher wavelengths (> 450 nm) and minimal changes in the spectral shapes when compared to spectra at lower concentration suggests lack of inter-chromophoric interactions even at higher concentrations.

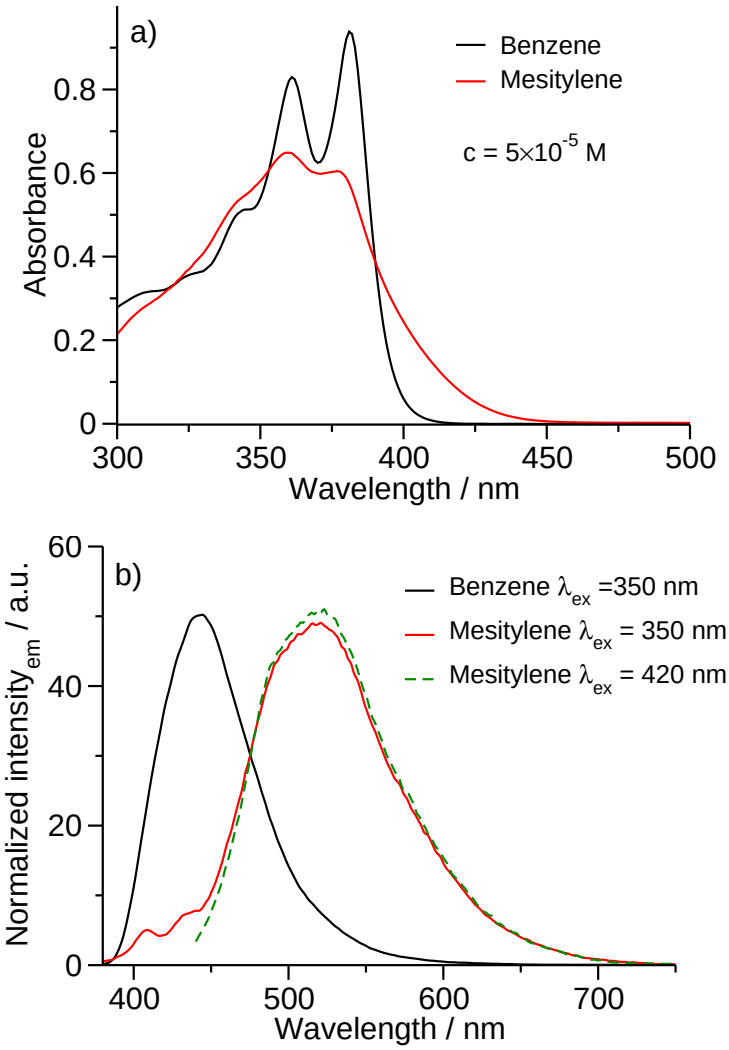

Figure S13: a) and b) UV/Vis absorption and emission spectra respectively of **NDI-Amph** (c = 5×10^{-5} M)

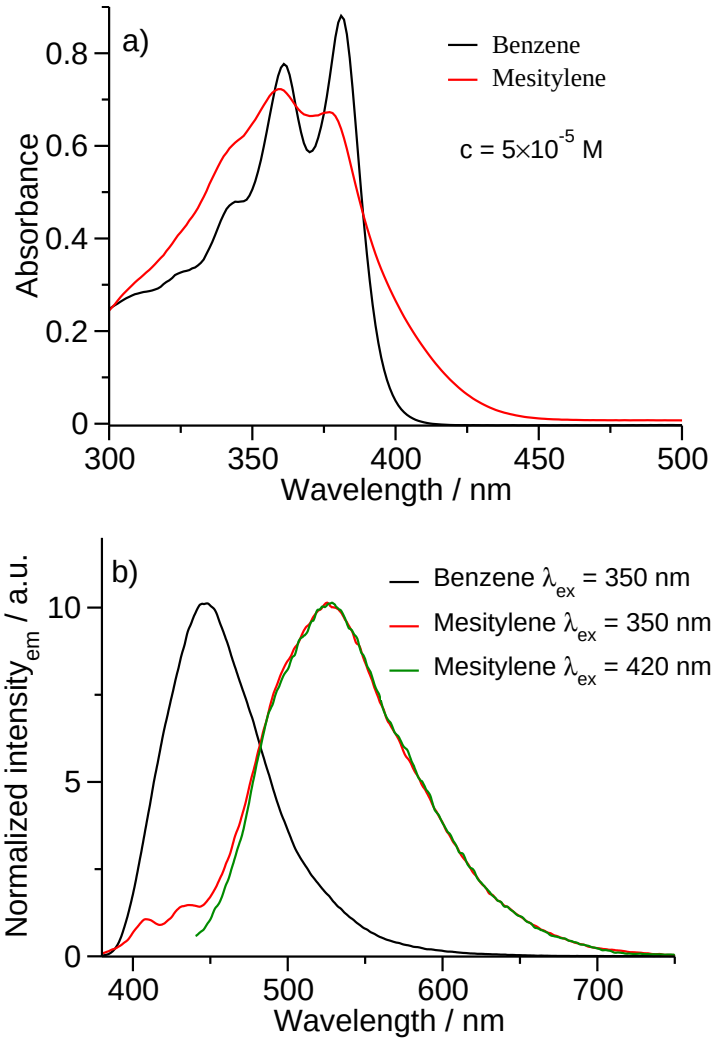

Figure S14: a) and b) UV/Vis absorption and emission spectra respectively of **NDI-Bolaamph** (c = 5×10^{-5} M)
As can be seen from emission spectra, even exciting at the CT band (>400 nm) also yields similar emission features. This again suggests that the emission is arising from ground-state charge-transfer (CT)

Molecule	Fluorescence quantum yield (Φ_f) in				
	o-DCB	Benzene	Toluene	*o*-Xylene	Mesitylene
2	0.0067	0.0628	0.0222	0.0208	0.0100
NDI-Bolaamph	0.0040	0.0153	0.0137	0.0127	0.0072
NDI-Amph	0.0044	0.0135	0.0129	0.0138	0.0077

Table S1: Fluorescence quantum yield (Φ_f) of different molecules in various aromatic solvents (c = 5×10^{-5} M)

Generally the fluorescence intensity quenches with the formation of charges-transfer complexes.[14] *The observed decrease in* Φ_f *from benzene to mesitylene (Table S1) points to stronger CT of NDIs with mesitylene leading to lower* Φ_f

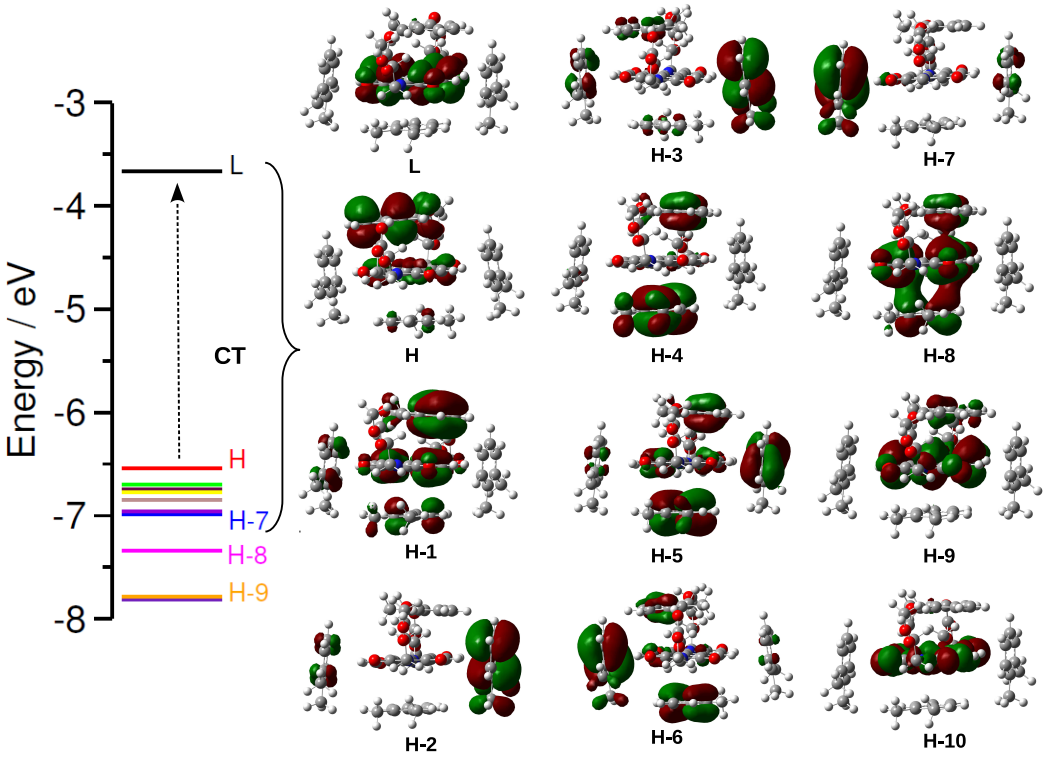

Figure S15: Frontier Molecular Orbital (FMO) diagram of the complex between model compound and four *o*-xylene molecules calculated at B3LYP-D3/DZVP//B3LYP/6-31+G(d,p) level of theory. The left panel indicates the energy level diagram and the corresponding FMOs are shown on the right hand side. Isovalue of 0.02 e(bhor)$^{-3}$ was used for molecular orbital plots. H and L stand for HOMO and LUMO respectively.
Transitions from HOMO-n (n = 0-7) to LUMO corresponds to the CT transitions. HOMO-n (n>7) to LUMO transitions corresponds mainly to the π-π^* transitions of the NDI chromophore.

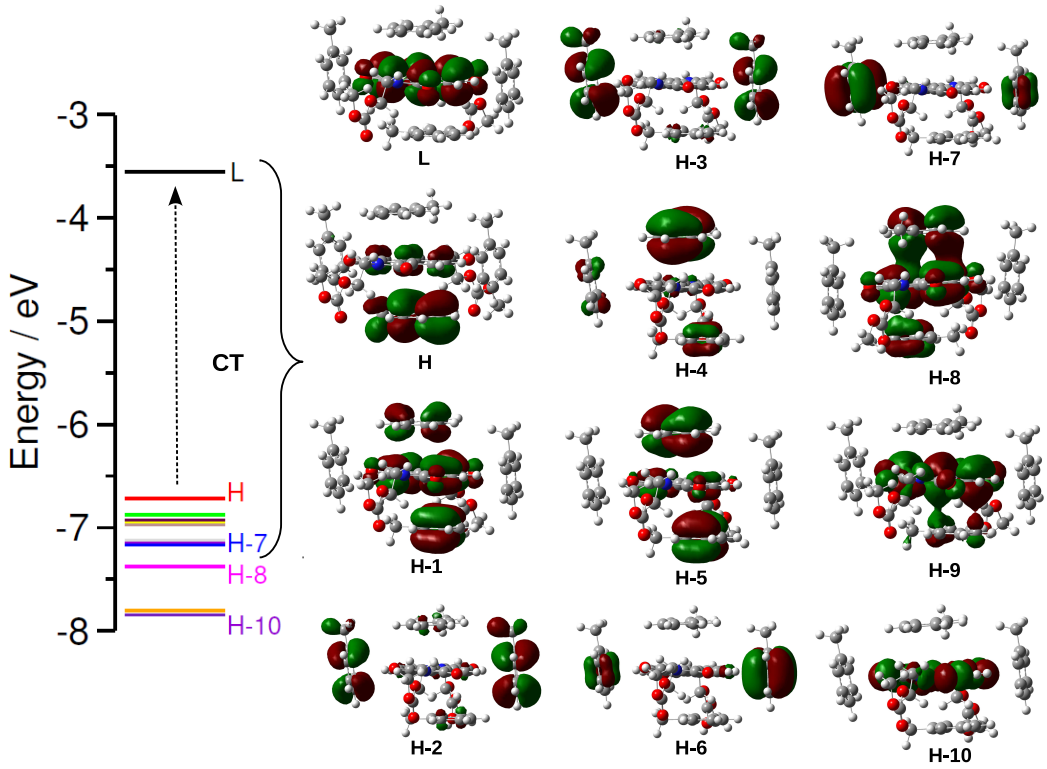

Figure S16: Frontier Molecular Orbital (FMO) diagram of the complex between model compound and four toluene molecules calculated at B3LYP-D3/DZVP//B3LYP/6-31+G(d,p) level of theory. The left panel indicates the energy level diagram and the corresponding FMOs are shown on the right hand side. Isovalue of 0.02 e(bhor)$^{-3}$ was used for molecular orbital plots. H and L stand for HOMO and LUMO respectively.
Transitions from HOMO-n (n = 0-7) to LUMO corresponds to the CT transitions. HOMO-n (n>7) to LUMO transitions corresponds mainly to the π-π^* transitions of the NDI chromophore.

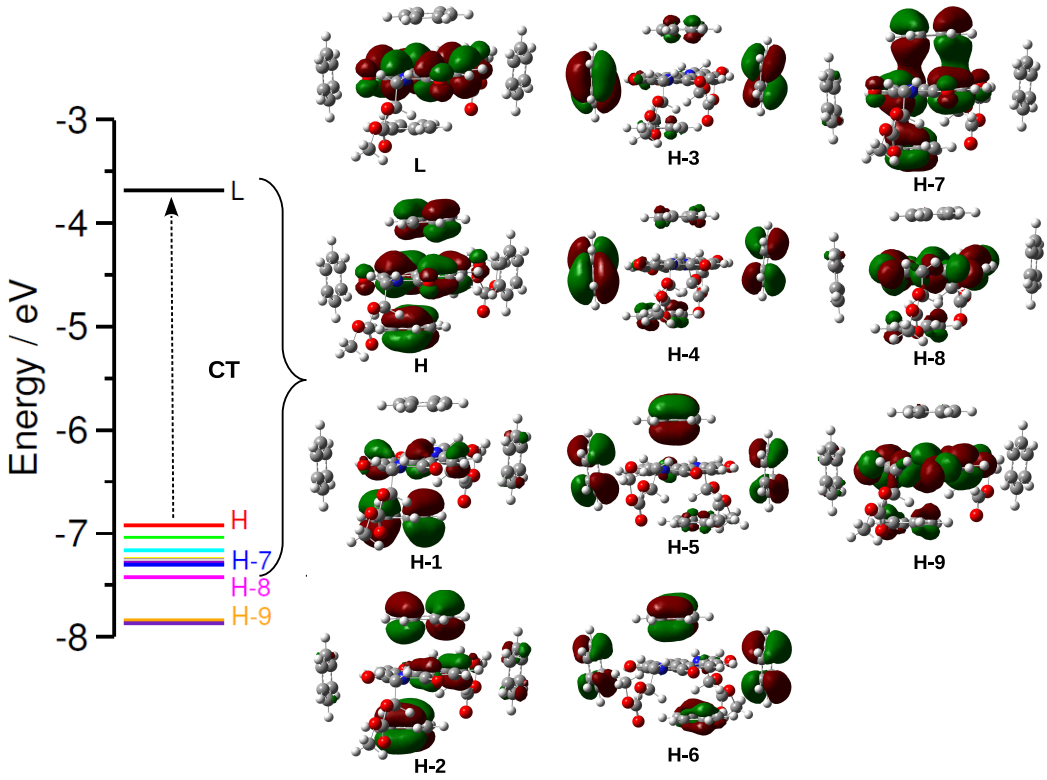

Figure S17: Frontier Molecular Orbital (FMO) diagram of the complex between model compound and four benzene molecules calculated at B3LYP-D3/DZVP//B3LYP/6-31+G(d,p) level of theory. The left panel indicates the energy level diagram and the corresponding FMOs are shown on the right hand side. Isovalue of 0.02 e(bhor)$^{-3}$ was used for molecular orbital plots. H and L stand for HOMO and LUMO respectively.
Transitions from HOMO-n (n = 0-7) to LUMO corresponds to the CT transitions. HOMO-n (n>7) to LUMO transitions corresponds mainly to the π-π^* transitions of the NDI chromophore.

4 Computed oscillator strengths of 1′ and 1′+four molecules of aromatics

Wavelength (nm)	Oscillator strength
577.95	0.0050
562.96	0.0059
533.96	0.0117
517.36	0.0005
510.09	0.0003
506.36	0.0001
493.44	0.0235
483.88	0.0073
388.79	0.1843
376.64	0.0006
360.00	0.0003
355.19	0.0210
331.70	0.0062
329.07	0.0001
323.61	0.0014
319.26	0.0029
311.06	0.0006
309.15	0.0024
307.37	0.0770
301.97	0.0164
298.50	0.0007
297.28	0.0001
295.68	0.0000
292.95	0.0001

Table S2: Vertical transitions for NDI+mesitylene complex

Wavelength (nm)	Oscillator strength
543.07	0.0117
501.20	0.0186
488.21	0.0034
477.80	0.0108
471.13	0.0078
462.72	0.0173
444.26	0.0107
437.22	0.0044
381.40	0.0128
377.90	0.1615
363.74	0.0003
350.88	0.0119
333.49	0.0064
330.52	0.0001
313.85	0.0007
312.08	0.0020
308.13	0.0671
301.94	0.0067
299.86	0.0010
292.46	0.0002
291.87	0.0161
287.04	0.0005
285.56	0.0018
283.50	0.0015

Table S3: Vertical transitions for NDI+*o*-xylene complex

Wavelength (nm)	Oscillator strength
507.55	0.0112
466.98	0.0011
464.34	0.0302
446.57	0.0312
441.20	0.0046
435.22	0.0159
417.88	0.0000
413.35	0.0006
379.13	0.0444
377.47	0.1364
361.92	0.0006
349.89	0.0109
332.41	0.0066
328.74	0.0002
311.02	0.0034
305.91	0.0667
301.13	0.0079
298.35	0.0005
293.88	0.0019
293.72	0.0003
284.26	0.0143
279.67	0.0000
277.06	0.0054
275.53	0.0002

Table S4: Vertical transitions for NDI+Toluene complex

Wavelength (nm)	Oscillator strength
455.02	0.0350
449.08	0.0189
431.25	0.0194
418.75	0.0003
405.10	0.0002
403.13	0.0001
400.24	0.0431
394.98	0.0014
378.36	0.0111
374.65	0.1719
361.63	0.0003
345.95	0.0038
331.85	0.0067
328.51	0.0002
310.22	0.0005
305.44	0.0735
298.37	0.0010
292.93	0.0002
292.11	0.0007
281.23	0.0028
279.81	0.0000
274.40	0.0049
271.73	0.0004
270.58	0.0005

Table S5: Vertical transitions for NDI+benene complex

Wavelength (nm)	Oscillator strength
391.18	0.0150
382.76	0.3464
372.66	0.0004
354.22	0.0045
341.31	0.0066
339.32	0.0044
329.01	0.0016
322.55	0.0023
315.79	0.0024
312.59	0.0990
305.59	0.0000
295.19	0.0000
284.56	0.0000
282.20	0.0000
277.60	0.0001
260.60	0.0000
250.72	0.0000
244.66	0.0000
242.90	0.0002
237.68	0.0003
235.20	0.0146
235.14	0.2258
230.25	0.0454
226.45	0.0123

Table S6: Vertical transitions for NDI alone

References

[1] J. R. Lakowicz, *Principles of Fluorescence Spectroscopy*, Springer, 3rd edn, 2006.

[2] C. Reichardt, *Solvents and Solvent Effects in Organic Chemistry*, WILEY-VCH Verlag, 3rd edn, 2003.

[3] J. VandeVondele, M. Krack, F. Mohamed, M. Parrinello, T. Chassaing and J. Hutter, *Comp. Phys. Commun.*, 2005, **167**, 103 – 128.

[4] J. Hutter, M. Iannuzzi, F. Schiffmann and J. VandeVondele, *Wiley Interdiscip. Rev. Comput. Mol. Sci.*, 2014, **4**, 15–25.

[5] A. D. Becke, *J. Chem. Phys.*, 1993, **98**, 5648–5652.

[6] C. Lee, W. Yang and R. G. Parr, *Phys. Rev. B*, 1988, **37**, 785–789.

[7] J. VandeVondele and J. Hutter, *J. Chem. Phys.*, 2007, **127**, 114105–114114.

[8] S. Grimme, J. Antony, S. Ehrlich and H. Krieg, *J. Chem. Phys.*, 2010, **132**, 154104.

[9] C. Hartwigsen, S. Goedecker and J. Hutter, *Phys. Rev. B*, 1998, **58**, 3641–3662.

[10] S. Goedecker, M. Teter and J. Hutter, *Phys. Rev. B*, 1996, **54**, 1703–1710.

[11] R. Byrd, P. Lu, J. Nocedal and C. Zhu, *J. Sci. Comput.*, 1995, **16**, 1190–1208.

[12] M. J. Frisch, G. W. Trucks, H. B. Schlegel, G. E. Scuseria, M. A. Robb, J. R. Cheeseman, G. Scalmani, V. Barone, B. Mennucci, G. A. Petersson, H. Nakatsuji, M. Caricato, X. Li, H. P. Hratchian, A. F. Izmaylov, J. Bloino, G. Zheng, J. L. Sonnenberg, M. Hada, M. Ehara,

K. Toyota, R. Fukuda, J. Hasegawa, M. Ishida, T. Nakajima, Y. Honda, O. Kitao, H. Nakai, T. Vreven, J. A. Montgomery, Jr., J. E. Peralta, F. Ogliaro, M. Bearpark, J. J. Heyd, E. Brothers, K. N. Kudin, V. N. Staroverov, R. Kobayashi, J. Normand, K. Raghavachari, A. Rendell, J. C. Burant, S. S. Iyengar, J. Tomasi, M. Cossi, N. Rega, J. M. Millam, M. Klene, J. E. Knox, J. B. Cross, V. Bakken, C. Adamo, J. Jaramillo, R. Gomperts, R. E. Stratmann, O. Yazyev, A. J. Austin, R. Cammi, C. Pomelli, J. W. Ochterski, R. L. Martin, K. Morokuma, V. G. Zakrzewski, G. A. Voth, P. Salvador, J. J. Dannenberg, S. Dapprich, A. D. Daniels, . Farkas, J. B. Foresman, J. V. Ortiz, J. Cioslowski and D. J. Fox, *Gaussian 09 Revision D.01*, Gaussian Inc. Wallingford CT 2009.

[13] R. Dennington, T. Keith and J. Millam, *GaussView; Version 5.0*, Semichem Inc.: Shawnee Mission, KS, 2009.

[14] M. D. Gujrati, N. S. S. Kumar, A. S. Brown, B. Captain and J. N. Wilson, *Langmuir*, 2011, **27**, 6554–6558.